

Algorithm for image-based biomarker detection for differential diagnosis of Parkinson's disease

Gurpreet Singh*, Lakshminarayanan Samavedham**

*Department of Chemical and Biomolecular Engineering,
National University of Singapore, Singapore, 117585*

***Correspondence to: Lakshminarayanan Samavedham*

E-mail: laksh@nus.edu.sg; Tel: +65-65165802

** E-mail: gurpreet@u.nus.edu;*

Abstract: The necessity is greater than ever for a methodology to both diagnose at early stage and evaluate the progression of Parkinson Disease (PD). In this paper, we propose an interesting and innovative methodology for pattern recognition based automated individual-level clinical diagnosis of PD. It makes use of a unique combination of machine learning tools and statistical tools. The methodology comprises of three major steps. First, pre-processed brain Magnetic Resonance Images (MRI) are modelled using Self-Organizing Map (SOM) for feature generation. Second, Fisher-Discriminant Ratio (FDR) is used to reveal distinctive feature(s). Third, Least Squares Support Vector Machine (LS-SVM) is used for Individual-level patient classification. The applicability of the proposed methodology has been demonstrated using 831 T1-weighted MRIs obtained from Parkinson's Progression Markers Initiative (PPMI) database. We have achieved classification accuracy of up to 97% for differential diagnosis of PD with confidence interval of 99.9%. This method is particularly suited for diagnosing patients in early stages of the disease, i.e., patients in age of 31- 60 years. In the present landscape, Brain MRI is routinely performed to assist PD diagnosis in clinical settings. Thus, the induction of the proposed methodology as a decision support system could make a significant impact on treatment strategies especially by aiding early-stage disease diagnosis.

Keywords: Artificial Intelligence. Automatic recognition. Computer aided diagnosis. Decision Support systems. Image analysis. Machine Learning. Parkinson Disease. SOM Modelling. LSSVM

1. INTRODUCTION

Parkinson's disease (PD) is a progressive neurodegenerative condition associated with nigrostriatal dysfunction leading to abnormal motor and non-motor functions. It has currently affected over 10 million people worldwide. The prevalence of this disease is especially on rise in developed nations like America and Singapore where as many as 1 and 0.3 million people respectively, live with PD. This is more than the number of people identified with Amyotrophic lateral sclerosis (ALS), multiple sclerosis (MS), and muscular dystrophy (MD) combined together. As per the statistical estimates in America, each year about 60,000 new PD cases are recorded and in addition to this number, thousands of cases go undetected. It is also expected that this number will further rise in countries with ageing population (such as Singapore and America) as the incidence of Parkinson's increases with age (Tan et al. 2004).

Currently, there is no definitive test for diagnosis of PD. Clinical diagnosis is mainly based on manual assessment of patient's history and valuation of his/her observable signs and symptoms. In early PD, clinical assessment is challenging as all the clinical signs and symptoms may not yet be manifested (Hughes et al. 2002). Further, distinguishing early PD from other similar conditions such as Scans without evidence for dopaminergic deficit (SWEDD) subjects is not only challenging but also important to prevent improper drug

diagnosis. Histological examination of substantia nigra region in the brain for lewy body accumulation is the only method for confirmative diagnosis of PD, which is clearly impractical during life.

Neuroimaging literature suggests that greater precision can be achieved by incorporating the use of neuroimaging for PD diagnosis. As the focus shifts from studying brain regions at group-level to Individual-level patient classification, multivariate analysis tools such as machine learning tools are increasingly being employed for analysing neuroimaging data. In a typical MRI, anatomical alterations due to degeneration of cells in the brain appear as areas with intensity variation. New algorithms, by combining different machine learning algorithms, are increasingly being developed to extract information about specific brain structure(s) that become consistently affected in a given disease to assist in automated subject classification (Dyrba et al. 2013; Padilla et al. 2012; Salvatore et al. 2014).

In this study, we propose an innovative and effective approach for monitoring disease progression and clinical diagnosis of PD which is based on combination of two machine learning algorithms viz., (1) An unsupervised, Self-Organising Map (SOM) and (2) A supervised learning based Least Squares Support Vector Machine (LSSVM).

2. MATERIALS AND METHODS

2.1 Study Participants

We obtained morphological T1-weighted Magnetic Resonance Images (MRIs) of SWEDD, PD and Healthy Control (HC) subjects from PPMI database. PPMI is a five year observational, international, multi-centre study aimed at understanding disease etiology by identifying PD progression biomarkers (Parkinson Progression Marker 2011). Clinical information on severity of the PD symptoms was assessed by Unified Parkinson's Disease Rating Scale (MDS-UPDRS) and the Hoehn and Yahr Scale. The Montreal Cognitive Assessment (MoCA) test was used for cognitive assessment of the subjects. Table 1 shows the demographic and clinical details of the subjects that comprise the dataset used in this work. For latest information, see www.ppmi-info.org.

Table 1: Demographic and clinical details of subjects.

Variables	HC	PD	SWEDD
N	245	518	68
M/F	155/90	346/172	48/20
Age	60.09 ± 11.35	61.79 ± 9.58	61.53 ± 10.59
Education	15.96 ± 2.87	15.43 ± 2.94	14.85 ± 3.88
MoCA	27.65 ± 1.51	26.62 ± 2.35	26.37 ± 2.32
H&Y	-	1.71 ± 0.39	1.35 ± 0.60
MDS-UPDRS	-	37.37 ± 13.41	28.93 ± 18.18

Note: Data are presented as Mean ± Standard Deviation.

MoCA, Montreal Cognitive Assessment; H&Y, Hoehn and Yahr scale; MDS-UPDRS, Movement Disorder Society- Unified Parkinson's Disease Rating Scale.

2.2 Study Design

Initially, entire dataset was divided into 6 Age-Unrelated Groups (AUG) based on clinically identified disease classes and brain matter i.e. WM and GM, see [Appendix A](#). For each classification group, 80 % of the images were used for preparing training dataset and rest 20 % were used during the testing phase. By using all the images from training dataset for a chosen classification group, an image representing voxel intensity changes (VIC) was created by subtracting the mean images two classes under consideration.

$$\mu_i = \frac{1}{N} \sum_{k=1}^N (I_k^i) \quad (1)$$

Here, μ_i denotes the i^{th} class mean image. N refers to the number of images and I_k^i refers to k^{th} image in the i^{th} class.

$$I_{\text{Dab}} = \mu_a - \mu_b \quad (2)$$

Here, I_{Dab} is VIC image corresponding to classification group formed by subtracting mean images, μ_a and μ_b of subject class a and b respectively. Here a can be HC/PD and b can be PD/SWEDD.

But, Progression of PD occurs in an age dependent manner. We intended to divide entire ensemble of images for each class of patients into Age-Related Subgroups (ARS) such that each subgroup represents patients of similar age and at a comparable stage of the disease. A total of 32 age-related subgroups were created by considering an age-range of 10 years (For example, patients aged 30-40, 40-50 years and so on), see Figure 1. (Please note: There were no SWEDD patients of age > 80.) For these classification groups, as the subjects should be at comparable stage of disease, we expected that the accuracy of classification should be better in comparison to that obtained on applying the devised methodology on AUG. The results obtained upon using AUG have been compared with those using ARS approach in Section 3.3. We have made tissue-by-tissue comparison between Healthy Control, PD and SWEDD subjects. For each run dataset was randomly divided into 10 folds. Out of this, 80 percent of the images were used for training the classifier model and the rest 20 percent were only used for testing the classification accuracy.

2.3 Image Pre-processing

All the steps concerning image pre-processing and segmentation of Brain MRI were performed using VBM8 toolbox for SPM8 on Brain MRI dataset obtained from PPMI database. Pre-processing involved skull-stripping and spatial normalization of images. Thereafter all the images were co-registered to ICBM template before they were segmented into Grey matter (GM) and White Matter (WM). The whole procedure was performed using 'Estimate and Write' option in the VBM8 toolbox (Kurth et al. 2010) for Statistical Parametric Mapping (SPM) (Friston 2003) software v8.

2.4 Feature Extraction

Self-Organizing Map (SOM) has been used for vector quantization and feature extraction from pre-processed VIC image for each classification group. SOM is a biologically inspired non-parametric unsupervised clustering algorithm based on competitive learning. It has a unique advantage of generating spatially organized representation along with vector quantization of input data. In this algorithm, number of neurons in the input layer is equal to the dimensionality of the input data (vectors in feature space) whereas output layer contains automatically selected or user-defined number of neurons arranged in a topographical grid. A high-dimensional input feature space can be quantized to low dimensional map points known as best matching units (BMUs) in an output space while still preserving the topographical relations present in the input data. SOM training algorithm has 2 steps

1. Competition amongst the neurons in output layer to determine BMUs (also called the winning neuron). This is also referred to as vector quantization of input data vectors that is based on similarity and squared Euclidean distance amongst the prototype vector and input data instance.

$$\|x_n - m_c\| = \min \|x - m_i\| \quad (3)$$

2. Neurons in the output layer are topographically related subsets that are updated after every input data instance based on lateral interaction between them.

$$m_i(t+1) = m_i(t) + h_{ci}(t) [x_n(t) - m_i(t)] \quad (4)$$

$$h_{ci}(t) = \exp\left(-\frac{d_{ci}^2}{2\sigma_i^2}\right) \quad (5)$$

Where x_n is n^{th} sample from input space, m_c is the reference vector closest to x_n , m_i is i^{th} reference vector from output space, h_{ci} is the kernel function that defines the neighborhood around BMU (here m_c).

These steps are carried out iteratively resulting in an ordered organization of data in the output space even from disordered data in the input space, aptly called self-organizing map. Beside its robustness to deal with high dimensional datasets, it also allows simultaneous visualization and clustering based on the topological pattern of input space. This results into a representation of the input space to discrete low dimensional map points known as best matching units (BMUs) in an output space while still preserving the topographical relations present in the input data.

Pre-processed images contained 121x145x121 voxels. It was aimed to study differences between PD, SWEDD, normal subjects. For classification, it is required to choose voxels according to a specific discriminative criterion, which can be used as classifiers. To rank voxels as per their statistical significance Fisher Discriminant Ratio (FDR) criterion was used. This ratio is useful to reveal discriminant variables between classes. For two-class case, it is defined as follows:

$$I_p^{FDR} = \frac{(\mu_1 - \mu_2)^2}{(\sigma_1^2 + \sigma_2^2)} \quad (6)$$

Here, I_p^{FDR} image is created for a p^{th} classification group. μ_i and σ_i denote the i^{th} class mean (See Eq. 1) and variance images calculated as follows

$$\sigma_i = \frac{1}{N} \sum_{k=1}^N (I_k^i - \mu_i)^2 \quad (7)$$

Here, N refers to the number of images and I_k^i refers to k^{th} image in the i^{th} training set.

2.5 Feature selection

A total of 38 VIC Images were created by subtracting mean images of different classes to incorporate information about intensity into feature space for SOM training. (A total of 32 VICs for ARS approach and 6 VICs for AUG approach). For each VIC image, we created vectors that form feature space for Self-Organizing Map (SOM) based vector quantization. These vectors contained information about 3-D coordinates, intensity difference and FDR score for each image voxel.

$$X_n = (i, j, k, I_{Dab}, I^{FDR}) \quad (8)$$

Here, X_n is n^{th} sample from input feature space X , (i, j, k) are the coordinates of the voxel corresponding to VIC image with voxel intensity I_{Dab} and I^{FDR} .

Thereafter, we normalized each column of this feature space vector. The range of the first three columns representing the coordinates of the voxel was restricted within $[0, 1]$. For 4th and 5th column, z-score based normalization was applied. We chose a Gaussian kernel function and a cylindrical shape of output map. A sequential SOM training algorithm was applied to input feature space to obtain an output map containing 500 neurons. After SOM training, the first 3 columns were again de-normalized to visualize the exact location of the generated ROIs.

SOM toolbox v2.0 for MATLAB was obtained from Laboratory of Computer and Information Science (CIS). For more details, see (<http://www.cis.hut.fi/projects/somtoolbox>). Thereafter, features in every image in a classification group were ranked according to information obtained from BMUs for corresponding VIC image and FDR score at each voxel as follows

$$ROI_p^m = \sum_{(i,j,k) \in BMUS} I_m(i,j,k) * I_p^{FDR}(i,j,k) \quad (9)$$

Here, ROI_p^m refers to Regions of Interest and (i, j, k) are the coordinates at voxel corresponding to m^{th} image belonging to p^{th} classification group.

Thus, every image was reduced to a vector containing 500 ROIs. The feature that is most representative of the difference between two chosen classes will be ranked highest and vice-versa.

2.6 Individual-level Patient Classification

A decision support system for differential diagnosis must be able to categorically label an unseen MRI into predefined groups based on patterns learned from training data. Ranked data points obtained after feature selection were directly used to obtain training and test vectors. We created an n -dimensional vector consisting of $n \times 500$ data points, where n represents number of subjects. We present here the results obtained using Least Square Support Vector Machine (LSSVM) to determine the accuracy of patient classification. Least squares Support Vector Machine (LSSVM) based classification decodes discriminative patterns by distinctive feature selection and optimal hyper-plane interpretation (Suykens & Vandewalle 1999). Theoretically, LSSVM is a kernel based supervised learning method that allows categorization of data by non-linear mapping of the input vectors (SOM trained maps) to a very high dimensional feature space to create a linear separation surface that can separate the input vector classes.

3. EXPERIMENTAL RESULTS AND DISCUSSION

3.1 Visual analysis for regional differences in GM and WM

To evaluate regional differences between different classes, we started by creating VIC image for each classification group. Figure 2 show the VIC images of GM and WM for HC v/s PD

subjects using AUG approach. These VIC images were modelled using our methodology to generate ROIs and then subjected to feature selection. As each ROI represents a voxel volume, we backtracked corresponding 3D projection for each ROI by using BMUs information contained in the SOM model. Figure 2 shows the reconstructed 3D volume for GM and WM for HC v/s PD subjects just below the VIC image. Most important ROIs marked are labelled and shown separately.

We found that the areas marked as most important regions, using Talairach Client (Lancaster et al. 2000), correctly correspond to relevant brain areas for PD pathology as reported in literature such as Putamen (Griffiths et al. 1994; Kordower et al. 2013), Medial Dorsal Nucleus (Henderson et al. 2000; Planetta et al. 2013), Pulvinar (Diederich et al. 2014),

Posterior cingulate cortex (Brodmann area 23) (van Eimeren et al. 2009), Retrosplenial cortex (Brodmann area 29) (Nagano-Saito et al. 2004) for GM and Corpus Callosum (Galantucci et al. 2014), Limbic cortex (Hilker et al. 2004) for WM, See Figure 2G and 2H. Further, the present methodology effectively distinguishes between areas that have been reported to become up regulated for dopamine synthesis, such as Brodmann area 23 and 29 indicated in blue, from those where neuronal loss leads to atrophy, such as Corpus Callosum, Pulvinar etc., as compared to HC subjects. Similar experiments were performed using both AUG and ARS approach for differentiating HC v/s SWEDD and PD v/s SWEDD. Classification results for individual-level differential diagnosis using both the approaches have been discussed in the Section 3.3.

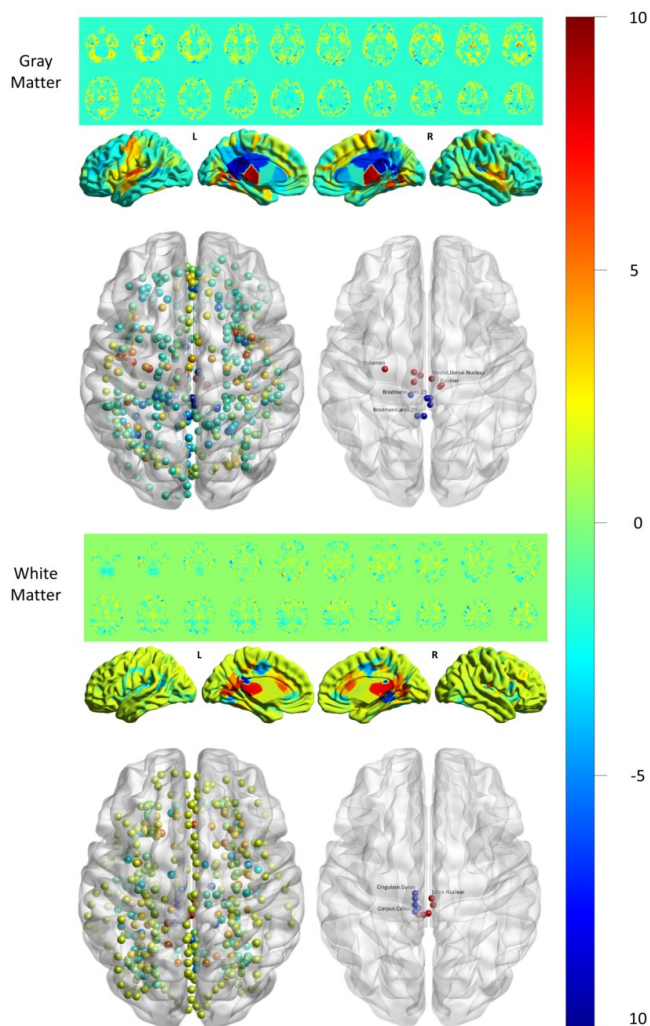


Figure 2: A Comparison of HC and PD subjects using VIC image and 3D Brain projection of ROIs generated using our methodology. We modelled VIC images for both GM and WM using SOM and subjected it to feature selection using FDR score. Most relevant ROIs were then labelled using Talairach Client (Lancaster et al. 2000). We found that the areas marked as most important regions correctly correspond to relevant brain areas for PD pathology as reported in literature. Using BMUs information contained in SOM volume, we backtracked the corresponding 3D projection for each ROI for each brain tissue.

3.2 Evaluation of Results

In addition to accuracy of prediction, four other statistical measures have been used to quantify the performance of the methodology used for patient classification. They are (1) Sensitivity or True Positive Rate (TPR) (2) Specificity or True Negative Rate (TNR) (3) Positive Predictive Value (PPV) (4) Negative Predictive Value (NPV). Table 2 shows the results for average classification accuracy with confidence interval at 99.9 %, obtained for both ARS and AUG approach, using proposed methodology. We performed multiple runs on these classification groups to check for consistency of classification accuracy. For every run, all the images belonging to a class were randomly selected for Training and Test sets.

3.3 Discussion and comparison with other methods

In the past, some efforts have been made to develop clinical decision support system by combining machine learning tools and statistical tools. Table 2 shows a comparison between accuracy for studies investigating the diagnostic potential of these methods for neuroimaging data. As per knowledge of the authors, using our methodology, highest accuracy of classification between HC v/s PD, PD v/s SWEDD and HC v/s SWEDD has been achieved. Initially, we applied this methodology to AUG approach. We achieved classification accuracy of 87.42 ± 1.19 , 96.43 ± 1.18 , 94.63 ± 0.58 for HC v/s PD, HC v/s SWEDD, PD v/s SWEDD respectively.

As we expected, on changing our approach to ARS, higher classification accuracy of 97.22 ± 1.06 , 99.35 ± 0.82 , 98.92 ± 0.66 was obtained for HC v/s PD, HC v/s SWEDD, PD v/s SWEDD respectively.

Differentiating PD and SWEDD is particularly challenging due to similarity in clinical features. Inclusion of SWEDD subjects as probable PD patients may result in unwanted side-effects from potentially harmful therapies. On using the methodology developed in this paper, we were not only able to distinguish these subjects but it is also possible to indicate key areas that may qualify as reliable biomarker.

Also, on comparing the results obtained on using AUG and ARS, classification accuracy increased in each case regardless of choice of feature selection criterion or feature classification algorithm. This further strengthens our postulate that for algorithms aimed at computer assisted disease diagnosis,

Table 2: Comparison of studies investigating clinical decision support system for diagnosis of PD

Comparison	Accuracy	N	TNR	TPR	NPV	PPV	Authors	
HC v/s PD	83.2	56	81.9	85.4	-	-	(Focke et al. 2011)	
HC v/s PSP	86.2	56	92.1	82.9	-	-		
PSP v/s PD	84.7	56	87.5	83.8	-	-		
PSP v/s PD	96.8	31	100	90	-	-	(Duchesne et al. 2009)	
MSA v/s PD	71.87	32	-	36.4	-	-		
HC v/s PD	n.s.	43	-	-	-	-		
PSP v/s PD	96.8	37	-	-	-	-	(Haller et al. 2012; Haller et al. 2013)	
MSA v/s PD	71.9	40	-	-	-	-		
HC v/s PD	87.42±1.19	763	94.7	71.9	86.5	87.8	Proposed Methodology	
HC v/s SWEDD	96.43±1.18	586	88.1	98.8	96.7	95.5		AUG
PD v/s SWEDD	94.63±0.58	313	60.7	99.2	94.9	91.1		ARS
HC v/s PD	97.22±1.06	763	98.9	93.4	97.3	97.2		
HC v/s SWEDD	99.35±0.82	586	97.2	1	99.2	1		
PD v/s SWEDD	98.92±0.66	313	95.7	99.5	99.3	96.8		

N, Number of subjects; TNR, True Negative Rate or Specificity; TPR, True Positive Rate or Sensitivity; NPV, Negative Predictive Value; PPV, Positive Predictive Value

HC, healthy controls; PD, Parkinson's Disease; PSP, Progressive Supranuclear Palsy; MSA, Multiple Systems Atrophy; SWEDD, Scans Without Evidence of Dopaminergic Deficit; n.s., non-significant result.

changes in brain in the case of neurodegenerative diseases, such as PD, should be studied in terms of changes that happen with age of the subject (or depending upon the availability of information, duration of disease) rather than studying symptoms observed in all age groups at once. It is worth mentioning here that for age group corresponding to 31-50 years, i.e. early PD, averaged classification accuracy was 99.35%, See [Appendix B](#). Presently in clinical settings, diagnosing PD at prodromal stages is rarely possible. This reemphasizes that the current methodology can be the ideal choice to be used as decision support system in clinical practice.

The main contributions from this study are mentioned as follows

1. Early-stage PD diagnosis is particularly challenging either due to complete absence or similarity in clinically observable signs and symptoms. In this regard, the present methodology has successfully achieved high classification accuracy (~99%) for patients in early stages of the disease, i.e., patients in age of 31- 50 years.
2. As per authors, this is the first study concerning PD where the applied methodology has achieved average classification accuracy of up to 97.22 % with 98.9 % specificity and 93.4 % Sensitivity. Also, this study makes the first attempt to distinguish SWEDD subjects from HC and PD.
3. Upon using this methodology for determining regions of interest, areas that are automatically labelled, are in accordance with brain regions affected in case of PD and SWEDD

These results highlight the efficiency of this methodology to select discriminative ROIs for classification of subjects using structural MRI. The applicability if this methodology is not restricted to PD or SWEDD only but can be easily extended to

include other neurodegenerative diseases such as Alzheimer's disease (AD), Mild Cognitive Impairment (MCI), Progressive supranuclear palsy (PSP) etc. Due emphasis should also be laid on the effectiveness and the applicability of this method for differential diagnosis in early stages of these disease.

4. CONCLUSION

Neurodegenerative diseases like PD and AD are beginning to become a substantive economic burden. Recently, the medicine and engineering communities have recognized the urgent need to understand this class of brain diseases. Various tools and methods from different fields are being brought together to build reliable disease progression models to expand knowledge about etiology of these disease. In this work, we present a novel methodology using machine learning tools, viz. SOM, LSSVM and FDR as statistical measure for determining most discriminative feature for differential diagnosis of PD and SWEDD

We have tested the developed methodology on T1-weighted images obtained from PPMI clinical repository. An average classification accuracy of 99.93±0.26 % has been achieved to distinguish HC, PD, and SWEDD subjects. As per authors' knowledge, this is the highest reported accuracy for a PD diagnosis till date. Moreover, most relevant ROIs computed using this method are in agreement with areas that appear in literature as representative regions of PD.

This methodology could not only aid in diagnosing early PD but also be used for exploratory research corresponding to labelled ROIs yet not found in literature.

In this landscape, the present methodology could speed the evolution of evidence based prognosis within routine consultations for mitigating these diseases.

REFERENCES

Diederich, N.J. et al., 2014. Are patients with Parkinson's disease blind to blindsight? *Brain*. Available at:

- <http://brain.oxfordjournals.org/content/early/2014/04/24/brain.awu094.abstract>.
- Duchesne, S., Rolland, Y. & Verin, M., 2009. Automated computer differential classification in Parkinsonian Syndromes via pattern analysis on MRI. *Acad Radiol*, 16(1), pp.61–70. Available at: <http://www.ncbi.nlm.nih.gov/pubmed/19064213>.
- Dyrba, M. et al., 2013. Robust automated detection of microstructural white matter degeneration in Alzheimer's disease using machine learning classification of multicenter DTI data. *PLoS One*, 8(5), p.e64925. Available at: <http://www.ncbi.nlm.nih.gov/pubmed/23741425>.
- Van Eimeren, T. et al., 2009. Dysfunction of the default mode network in Parkinson disease: a functional magnetic resonance imaging study. *Arch Neurol*, 66(7), pp.877–883. Available at: <http://www.ncbi.nlm.nih.gov/pubmed/19597090>.
- Focke, N.K. et al., 2011. Differentiation of typical and atypical Parkinson syndromes by quantitative MR imaging. *AJNR Am J Neuroradiol*, 32(11), pp.2087–2092. Available at: <http://www.ncbi.nlm.nih.gov/pubmed/21998102>.
- Friston, K., 2003. Statistical Parametric Mapping. In R. Kötter, ed. *Neuroscience Databases*. Springer US, pp. 237–250. Available at: http://dx.doi.org/10.1007/978-1-4615-1079-6_16.
- Galantucci, S. et al., 2014. Corpus Callosum Damage and Motor Function in Parkinson's Disease (P2.006). *Neurology*, 82(10 Supplement), p.P2.006. Available at: http://www.neurology.org/content/82/10_Supplement/P2.006.abstract.
- Griffiths, P.D., Perry, R.H. & Crossman, A.R., 1994. A detailed anatomical analysis of neurotransmitter receptors in the putamen and caudate in Parkinson's disease and Alzheimer's disease. *Neurosci Lett*, 169(1-2), pp.68–72. Available at: <http://www.ncbi.nlm.nih.gov/pubmed/8047295>.
- Haller, S. et al., 2013. Differentiation between Parkinson disease and other forms of Parkinsonism using support vector machine analysis of susceptibility-weighted imaging (SWI): initial results. *Eur Radiol*, 23(1), pp.12–19. Available at: <http://www.ncbi.nlm.nih.gov/pubmed/22797981>.
- Haller, S. et al., 2012. Individual detection of patients with Parkinson disease using support vector machine analysis of diffusion tensor imaging data: initial results. *AJNR Am J Neuroradiol*, 33(11), pp.2123–2128. Available at: <http://www.ncbi.nlm.nih.gov/pubmed/22653326>.
- Henderson, J.M. et al., 2000. Loss of thalamic intralaminar nuclei in progressive supranuclear palsy and Parkinson's disease: clinical and therapeutic implications. *Brain*, 123 (Pt 7), pp.1410–1421. Available at: <http://www.ncbi.nlm.nih.gov/pubmed/10869053>.
- Hilker, R. et al., 2004. Subthalamic nucleus stimulation restores glucose metabolism in associative and limbic cortices and in cerebellum: evidence from a FDG-PET study in advanced Parkinson's disease. *J Cereb Blood Flow Metab*, 24(1), pp.7–16. Available at: <http://www.ncbi.nlm.nih.gov/pubmed/14688612>.
- Hughes, A.J. et al., 2002. The accuracy of diagnosis of parkinsonian syndromes in a specialist movement disorder service. *Brain*, 125(Pt 4), pp.861–870. Available at: <http://www.ncbi.nlm.nih.gov/pubmed/11912118>.
- Kordower, J.H. et al., 2013. Disease duration and the integrity of the nigrostriatal system in Parkinson's disease. *Brain*, 136(Pt 8), pp.2419–2431. Available at: <http://www.ncbi.nlm.nih.gov/pubmed/23884810>.
- Kurth, F., Lüders, E. & Gaser, C., 2010. VBM8 Toolbox Manual.
- Lancaster, J.L. et al., 2000. Automated Talairach atlas labels for functional brain mapping. *Hum Brain Mapp*, 10(3), pp.120–131. Available at: <http://www.ncbi.nlm.nih.gov/pubmed/10912591>.
- Nagano-Saito, A. et al., 2004. Cognitive- and motor-related regions in Parkinson's disease: FDOPA and FDG PET studies. *Neuroimage*, 22(2), pp.553–561. Available at: <http://www.ncbi.nlm.nih.gov/pubmed/15193583>.
- Padilla, P. et al., 2012. NMF-SVM based CAD tool applied to functional brain images for the diagnosis of Alzheimer's disease. *IEEE Trans Med Imaging*, 31(2), pp.207–216. Available at: <http://www.ncbi.nlm.nih.gov/pubmed/21914569>.
- Parkinson Progression Marker, I., 2011. The Parkinson Progression Marker Initiative (PPMI). *Prog Neurobiol*, 95(4), pp.629–635. Available at: <http://www.ncbi.nlm.nih.gov/pubmed/21930184>.
- Planetta, P.J. et al., 2013. Thalamic projection fiber integrity in de novo Parkinson disease. *AJNR Am J Neuroradiol*, 34(1), pp.74–79. Available at: <http://www.ncbi.nlm.nih.gov/pubmed/22766668>.
- Salvatore, C. et al., 2014. Machine learning on brain MRI data for differential diagnosis of Parkinson's disease and Progressive Supranuclear Palsy. *J Neurosci Methods*, 222, pp.230–237. Available at: <http://www.ncbi.nlm.nih.gov/pubmed/24286700>.
- Suykens, J.A.K. & Vandewalle, J., 1999. Least Squares Support Vector Machine Classifiers. *Neural Processing Letters*, 9(3), pp.293–300. Available at: <http://dx.doi.org/10.1023/A%3A1018628609742>.
- Tan, L.C. et al., 2004. Prevalence of Parkinson disease in Singapore: Chinese vs Malays vs Indians. *Neurology*, 62(11), pp.1999–2004. Available at: <http://www.ncbi.nlm.nih.gov/pubmed/15184604>.